Experimental demonstration of robust spatial-diversity combining for coherent free-space optical transmission

Abraham Johst[1,2], Markus Nölle[1], Lutz Molle[1], Nicolas Perlot[2], Michael Rohde[3], Ronald Freund[2,4]
[1] Hochschule für Technik und Wirtschaft Berlin, Wilhelminenhofstraße 75A, 12459 Berlin, Germany;
[2] Fraunhofer Institute for Telecommunications HHI, Einsteinufer 37, 10587 Berlin, Germany;
[3] Berliner Hochschule für Technik, Luxemburger Straße 10, 13353 Berlin, Germany;
[4] Technical University of Berlin, Straße des 17. Juni 135, 10623 Berlin, Germany
abraham.johst@htw-berlin.de

Abstract: Spatial-diversity schemes are applied to improve signal quality of coherent free-space optical transmission systems with uncorrelated phase noise. We compare the performance of conventional schemes (MRC, SDC) to a newly proposed one (X-MRC).

1. Introduction

Coherent free-space optical (FSO) transmission systems have been an active research area in recent years [1]. However, these systems face the challenge of atmospheric turbulences, which causes bit errors due to strong signal power fluctuations. Promising solutions to overcome this behavior are adaptive optics [2] or multi-aperture arrays using spatial diversity to improve signal quality [3]. For such systems, numerical investigations [4], experimental demonstrations using CW signals [5] and optical link emulation [6] have been demonstrated so far. In this contribution we propose a new coherent combining approach and verify its feasibility to improve signal quality in both, numerical simulations and by transmission experiments over a 3.4 km free space link. We show that digital coherent combining can be realized even in the case of uncorrelated phase noise due to multiple different local oscillators used at the individual apertures, as they are required in a 4×1 MISO concept as proposed in [7]. Further, we demonstrate that the proposed combining approach is able to reduce computational DSP effort compared to the standard maximal-ratio combining (MRC) method, while obtaining equal outage probability of the system.

2. System setup

The system setup for both the simulations and the experimental study is shown in Fig. 1. The transmitter DSP generates a root-raised cosine pulse-shaped (roll-off of 0.1) single-polarization 12.8-GBd QPSK signal. The channel simulation consists of four parallel random realizations of lognormal distributed SNR values (corresponding to a scintillation index of 0.9) and random timing offsets per aperture, a static frequency offset of 100 MHz for all apertures, and uncorrelated phase noise processes (corresponding to a laser linewidth of 200 kHz) per aperture. The receiver DSP performs symbol timing recovery, carrier frequency offset (CFO) correction [8], SNR estimation based on the spectra of the individual received signals, aperture signal timing alignment and matched filtering. The subsequent carrier phase recovery (CPR) is implemented as dual stage algorithm to cope with potential cycle slips [9] and is performed independently on each aperture signal before combining. The first stage uses a pilot-based interpolation method [10] with a 1% pilot rate and acts as a coarse phase noise correction, while the second stage implements a blind phase search algorithm [11]. In addition to the conventional maximal-ratio combining and selection-diversity combining (SDC) schemes [12], a modified X-out-of-MRC (X-MRC) combining method optimized for low computational cost is proposed and investigated. The proposed method utilizes the information from the SNR estimation stage to only use the minimum required number of aperture signals for MRC combining in order to ensure a BER performance of the combined signal below the assumed FEC threshold of $5{\cdot}10^{-3}$ [13]. No further DSP needs to be performed on the remaining aperture signals, thus saving computational effort and power consumption.

Furthermore, the parameters of the DSP blocks that follow the SNR estimation are also set based on the estimated current SNR of each aperture signal. To judge the signal quality of the combined signal in addition to the BER, also the SNR of the combined signal is estimated. This step is presumably not needed in a real system.

It is worth mentioning that the offline DSP is performed block-wise with block sizes of 250000 samples (corresponding to ≈10µs). Since the time constant of the scintillation process is much larger (in the region of milliseconds), the mean signal power and therefore the SNR is assumed to be constant within one DSP block. This assumption allows us to use of the same basic system setup and DSP for both, the simulations and the experimental investigations. However, additional resampling was necessary to match the sample rates of the ADC and the DSP.

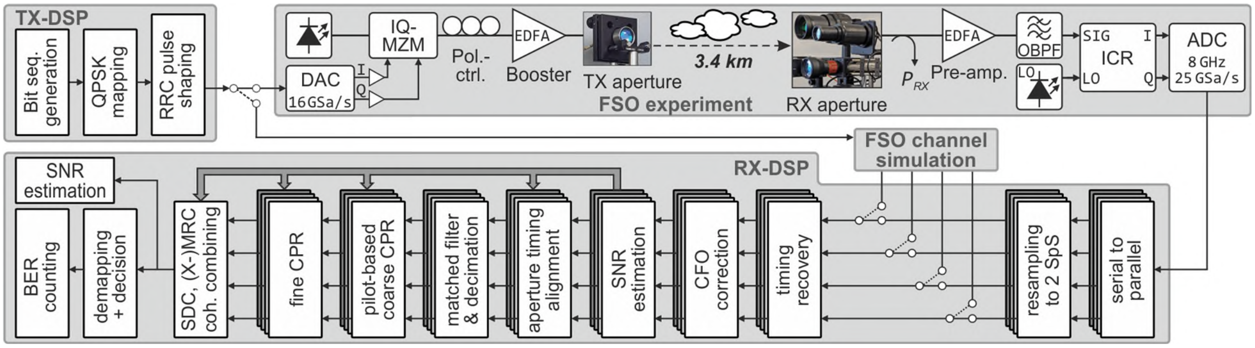

Figure 1: System setup. Experimental schematics on the upper right. Abbreviations: TX = Transmitter, RX = Receiver, RRC = root-raised cosine, DAC = digital-to-analog converter, MZM = Mach-Zehnder-Modulator, EDFA = Erbium doped fiber amplifier, OBPF = optical bandpass filter, LO = local oscillator, ICR = integrated coherent receiver, ADC = analog-to-digital converter, SpS = Sample per symbol.

3. Simulation results

To verify the combining principles and basic DSP performance in the given scenario, a simulation with 12000 Monte-Carlo runs was performed. The resulting SNR distributions for the individual aperture signals, as well as for the differently combined signals are shown in Fig. 2a). In the histogram, statistically unreliable areas with 10 or fewer events are shaded green. The SDC signal shows a larger mean SNR and less variance than the individual aperture signals. MRC of all four aperture signals shows the largest mean SNR of all algorithms. Although the mean SNR of the X-MRC combined aperture signals is lower than for MRC-combined signals, it can clearly be seen that the distribution is asymmetric and almost strictly limited towards lower SNR values when approaching the minimum required SNR to stay below the FEC threshold (corresponding to 8.2 dB SNR selection threshold). If the combined SNR is below the threshold, the X-MRC uses all four aperture signals for combining and approaches the MRC case. For higher SNR values, the X-MRC algorithm uses less aperture signals for combining and eventually approaches the SDC case. Fig. 2b) shows the histograms of the evaluated BER for the same signals as in the SNR histograms discussed above. The same tendencies as for the SNR distributions can be observed. For the assumed FEC threshold, system outage probabilities p_{out} for the different signals can be calculated. The individual aperture signals (corresponding to a SISO system) show p_{out} >65%, which is decreased with SDC down to about 19%. With X-MRC and MRC, the outage probability is reduced to 0.2%. Such a huge improvement by the X-MRC algorithm is all the more surprising because evaluation of the number of used aperture signals within the X-MRC algorithm reveals that in more than 98% of the cases only one or two apertures were used for combining. Three apertures were used in only 1% and four apertures in 0.9%, respectively. This shows the potential of the X-MRC algorithm to save processing effort and power consumption compared to the MRC case while still reaching the same outage probability.

4. Experimental verifications

To verify the findings from the simulation, an experimental demonstration was performed on a 3.4 km free space link. On the transmitter, standard hardware for coherent transmission was used in addition to an optical aperture as shown in Fig. 1. The transmit polarization was manually adjusted to match the coherent receiver's polarization axis. The parameters of the receiver aperture and the implementation details of the optical tracking are described in [3]. The coherently received in-phase and quadrature signals are digitized with a real-time oscilloscope to store samples for further processing using offline DSP. To emulate a multi-aperture receiver terminal, 18548 electrical waveform blocks were captured during a measurement period of more than 45 hours. The receiver optical input power P_{RX} as a function of measurement time is shown in Fig. 2c). Four subsequently stored waveforms are used to emulate a receiver with four apertures, leading to 4637 different channel realizations. The waveforms were acquired about every 9s, which is long enough to safely assume uncorrelated scintillation processes and also short enough to assure equal channel statistics. Since the four waveforms were recorded subsequently, the phase noise signature from the transmitter laser and the local oscillator is uncorrelated in each aperture signal. Figure 2d) shows histograms of the SNR distributions of the received signals. It can be concluded from the histograms that the signals show a very low outage probability due to rather good channel conditions in the measurement. Therefore it was decided to digitally add noise with a constant power to all the received signals in order to artificially deteriorate the transmission performance and to test the combination methods under higher outage probability. The SNR distributions for all signals after noise addition are shown Fig. 2f). These SNR histograms basically show the same tendencies as in the simulations: the individual aperture signals show the lowest mean SNR values, followed by SDC, X-MRC and the MRC algorithm.

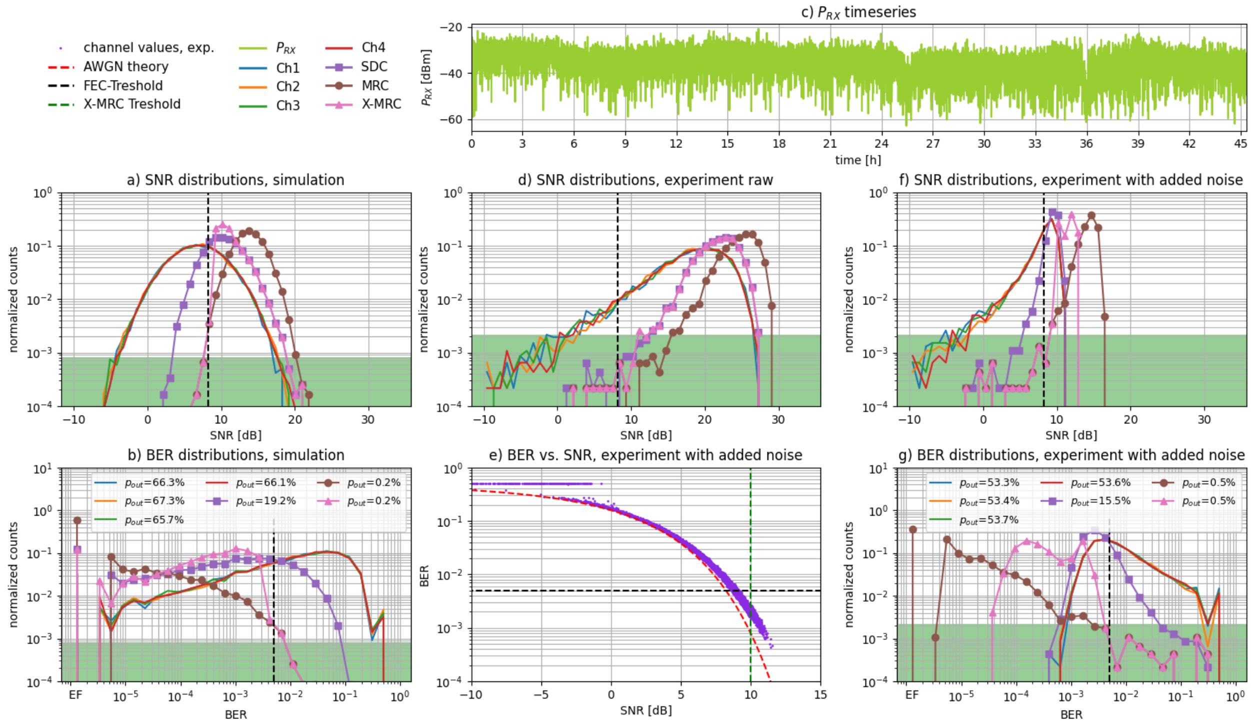

Figure 2: Results on simulation and experiment. Green marked area: less or equal 10 absolute counts, therefore statistically not reliable.

The related BER-vs-SNR performance of the individual channels as shown in Fig. 2e) is mostly in line with AWGN theory down to low SNRs. To cope with additional implementation penalty, the SNR-based selection threshold is adapted to 10 dB for X-MRC, as indicated Figure 2e). From BER histograms in Fig. 2g) it can be derived that the outage probability decreases from >50% for single aperture signals down to 0.5% when X-MRC or MRC is used. In contrast, SDC only improves the outage probability to about 15.5%. Similar as in the simulations, the X-MRC algorithm only uses signals from three or four apertures in less than 2% of all cases. In the remaining 98%, either a single aperture signal or the combination of two aperture signals is sufficient for performance below the FEC threshold. This experiment demonstrates that by permitting a higher mean BER (yet below FEC threshold), the X-MRC algorithm still achieves a similar outage probability as the computationally more expensive standard MRC algorithm.

5. Conclusion

We experimentally demonstrated the possibility to coherently combine multiple aperture signals after a 3.4 km FSO transmission even if the signals experience uncorrelated phase noise signatures. Further, we showed that a large outage reduction (from 50% to 0.5%) is reachable. The proposed X-MRC algorithm achieves the same system outage probabilities as the MRC algorithm but requires the combination of less aperture signals in more than 98% of the cases. This suggests a large potential for reduction of computational effort.

Acknowledgement

This work was supported by the Institut für angewandte Forschung (IFAF) Berlin.

6. References

[1] F. P. Guiomar et al., Journal of Lightwave Technology, vol. 40, no. 10, pp. 3173-3186, 2022.
[2] Y. Horst et al., Light: Science & Applications 12, 153 (2023), doi: 10.1038/s41377-023-01201-7.
[3] P. Hanne et al., Proc. 24th ITG-Symposium, pp.137-140, 2023.
[4] N. Liu et al., Journal of Lightwave Technology, vol. 41, no. 18, pp. 5983-5990, 2023.
[5] D. J. Geisler, et al., Proc. SPIE 10096, 100960C, 2017.
[6] L. Wang et al., Optics Express, vol. 30, no. 5, pp. 7854-7869, 2022.
[7] N. Perlot et al., ICSOS 2019, doi: 10.1109/icsos45490.2019.8978966.
[8] M. Morelli et al., European Transactions on Telecommunications, vol. 9, no. 2, pp. 103-116, 1998
[9] M. Magarini et al., IEEE Photonic Technology Letters, vol. 24, no. 9, pp. 739-741, 2012.
[10] A. Spalvieri et al., Research Letters in Communications, vol. 2009, doi: 10.1155/2009/645615.
[11] T. Pfau et al., Journal of Lightwave Technology, vol. 27, no. 8, pp. 989-999, 2009.
[12] D. Brennan, Proc. IRE, vol. 47, no. 6, pp. 1075-1102, 1959.
[13] D. A. de Arruda Mello et al., Digital Coherent Optical Systems, Springer, 2021.